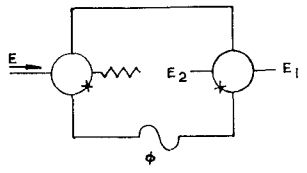

Fig. 1—Simple frequency discriminator.

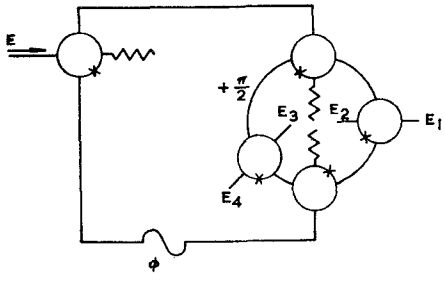

Fig. 2—Quadrature frequency discriminator.

Several advantages of the arrangement may be quoted:

1) An (r, θ) display can be used so that $\theta \propto \phi \propto f$.
2) Using an (r, θ) display, θ continuously and linearly increases with frequency over any range, although, of course, ambiguities occur in a range of ϕ exceeding 2π. "Clock" systems to give increased accuracy without ambiguity are possible. In this context, frequency ranges representing $2n\pi < \phi < 2(n+1)\pi$ of 10 Mc and 10,000 Mc are equally practicable.
3) $|E_1|^2 - |E_2|^2 \simeq |E_1| - |E_2|$ when $E_1 = \cos \phi/2$ and $E_2 = \sin \phi/2$ so that errors due to departure from square law in the detector characteristics are very small.
4) The subtraction $|E_1|^2 - |E_2|^2$ may be written

$$(E'^2 + E''^2 + 2E'E'' \cos\phi) - (E'^2 + E''^2 - 2E'E'' \cos\phi) = 4E'E'' \cos\phi$$

where E' and E'' are the input voltages to a phase-measuring hybrid junction, and $E' \neq E''$. It may be shown that the product $(E'E'')$, for both the phase measuring junctions, shown in Fig. 2, is not dependent upon equality of power split in the power dividing junctions and that therefore this equality is not necessary for good frequency measuring performance.

It should be noted that the four-junction circuit, giving the sine and cosine terms, is the same as that for a single-sideband modulator and is one of a large family of multiport networks that might be used in phase comparison applications. For example, an eight detector device giving $\cos\phi$, $\cos(\phi + \pi/4)$, $\cos(\phi + \pi/2)$ and $\cos(\phi + 3\pi/4)$ outputs can easily be realized. Such an arrangement shows improved measuring accuracy by removing quadrantal error terms.

STEPHEN J. ROBINSON
Systems Division
Mullard Research Labs.
Redhill, Surrey, England

Harmonic Generation by an Array

In the millimeter region, harmonic generators have long served as convenient signal sources. However, the power handling capacity of the diode elements is very limited. At the short-wave end of the millimeter spectrum, the dominant mode waveguide terminal of a harmonic generator may also be less desirable than a quasi-optical or beam output. These factors have led to the investigation of a diode array as a millimeter wave source. The results obtained show that such an array is feasible but uneconomic with presently available diodes.

A schematic diagram of a harmonic array is shown in Fig. 1. The fundamental power illuminates an array of receiving apertures from a feed horn which may be extended (as shown by the broken lines) to shield the entire input region, if desired. Depending on the spacing between feed and array, it may be necessary to introduce phase correction by means of a lens, or by changing the lengths of input waveguide in each multiplier unit. These units consist of a receiving or input horn coupled to an inline harmonic generator. The output guide is proportioned to pass only the desired harmonic and higher terms which are neglected. Each output horn occupies the same cross section as the corresponding input aperture. This provides grating lobe suppression, since a narrower element pattern compensates for the wider spacing at the output frequency. The output is in the form of a beam, which can be brought to a focus by choosing the proper phase correction on either the input or output side of the array.

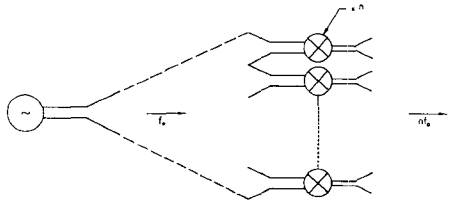

Fig. 1—Harmonic array.

To investigate the properties of a harmonic array, a 2×5 element array was constructed for $f_0 = 25$ Gc, $n = 2$. A very simple straight-through element, as shown in Fig. 2, was used. The individual crystals produced an input VSWR between 4:1 and 6:1 in this mount. Measurements on individual elements showed that the standard deviations in insertion phase shift and conversion loss were less than 25° and 1.7 db respectively for the 27 individual 1N26 crystals tested. The harmonic output of the array was within 1 db of the output calculated for the sum of the individual elements, each with the measured VSWR, and illumination corrections applied. It was therefore concluded that a harmonic array functions as a true additive structure. The array is shown in Fig. 3.

Manuscript received December 10, 1963. The work described here was performed under Contract No. AF 19 (628)-397 for the Air Force Cambridge Research Laboratories, Bedford, Mass.

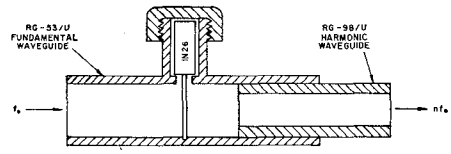

Fig. 2—Harmonic array element.

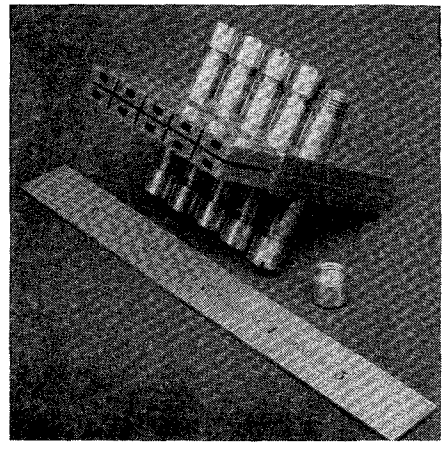

Fig. 3—Ten element harmonic array.

The performance of the experimental array shows conversion and coupling losses of about 20 db and 6 db respectively. With provisions for impedance matching in the elements, and with more efficient harmonic generators, a useful array source for millimeter and possibly submillimeter power might be constructed.

D. D. KING
F. SOBEL
J. W. DOZIER
Research Div.
Electronic Communications, Inc.
Timonium, Md.

Analogous Propagation Modes in Inhomogeneous Plasma and Tapered Waveguide

An interesting analogy exists between the propagation of transverse electromagnetic (TE) waves in a plasma (with no magnetic field) and in conventional waveguide.[1,2] This analogy reflects the similar roles played by the volume conduction current in the plasma and the wall conduction current in the waveguide and is of interest in that it provides insight into plasma propagation and suggests the possibility of simulating

Manuscript received July 19, 1963; revised December 16, 1963. This work was performed under the auspices of the U. S. Atomic Energy Commission.

[1] V. L. Ginzburg, "Propagation of Electromagnetic Waves in Plasma," Gordon and Breach Publishers, Inc., New York, N. Y.; 1962.
[2] W. Rotman, "Plasma simulation by artificial dielectrics and parallel-plate media," IRE TRANS. ON ANTENNAS AND PROPAGATION, vol. AP-10, pp. 82–95; January, 1962.

certain microwave properties of inhomogeneous plasma by means of appropriate waveguide configurations.

Consider a rectangular waveguide with short dimension (b) in the x direction, long dimension (a) in the y direction, and axis in the z direction. Propagation in the TE_{10} mode is described by the wave equation[3]

$$\frac{d^2E_x}{dz^2}+\left(\frac{\omega}{c}\right)^2\left[1-\left(\frac{\omega_c}{\omega}\right)^2\right]E_x=0 \quad (1)$$

where the cutoff frequency $\omega_c=\pi c/a$ and c is the velocity of light.

Similarly, propagation of a TE wave in the z direction in an infinite plasma is described by the equation[4]

$$\frac{d^2E_x}{dz^2}+\left(\frac{\omega}{c}\right)^2\left[1-\left(\frac{\omega_p}{\omega}\right)^2\right]E_x=0 \quad (2)$$

where the plasma frequency $\omega_p=(4\pi ne^2/m)^{1/2}$. The plasma wave equation (2) is formally identical with the waveguide equation (1) with the plasma frequency ω_p playing the role of the cutoff frequency ω_c.

In what follows it will be found instructive to develop the equivalent transmission line for TE propagation in an infinite plasma. We first write the two Maxwell curl equations for a plane wave propagating in the z direction:

$$\frac{\partial H_y}{\partial z}=\left[\frac{4\pi}{c}\frac{ne^2}{m}\frac{i}{\omega}-\frac{i\omega}{c}\right]E_x;$$
$$\frac{\partial E_x}{\partial z}=\frac{i\omega}{c}H_y, \quad (3)$$

where use has been made of the relation $\partial j/\partial t=(ne^2/m)E$.[4] The equivalent line voltage V and current I are related to the electric and magnetic fields by appropriate constants of proportionality that are conventionally adjusted to make the average propagated power equal to the product of the equivalent voltage and current, but these constants need not be evaluated in the present case. Writing (3) in terms of V and I we obtain the equations

$$\frac{\partial I}{\partial z}=\text{const}\,\frac{i}{\omega c}(\omega_p^2-\omega^2)V; \quad \frac{\partial V}{\partial z}=\text{const}\,\frac{i\omega}{cz}I$$

which are to be compared with the standard transmission-line equations $\partial I/\partial z=-YV$ and $\partial V/\partial z=-ZI$. Evidently the admittance of the plasma Y can be represented by a parallel resonant circuit with equivalent capacity $C_{eq}=1/c$ and inductance $L_{eq}=c/\omega_p^2$. The equivalent transmission line for TE propagation in a plasma is shown in Fig. 1(b); for comparison the equivalent transmission line for a waveguide[5] is shown in Fig. 1(a).

The transmission line shown in Fig. 1(b) offers a simple interpretation for the phenomenon of plasma cutoff. When $\omega>\omega_p$ the displacement current exceeds the conduction current and the shunt member made up of the free-space capacitive susceptance and the plasma inductive susceptance is capacitive; in conjunction with the free-space inductive series member this

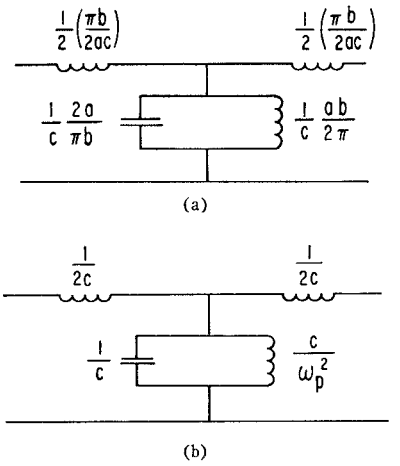

Fig. 1—Equivalent transmission lines. (a) For waveguide. (b) For plasma.

shunt member can support propagation. When $\omega<\omega_p$, however, the shunt member becomes inductive and the system can not support propagation.

Further insight into the analogy between plasma and waveguide propagation can be gained by examining the displacement current and the conduction current in the two cases (Fig. 1). In the waveguide case the transverse conduction current flowing in the walls is $-(2\pi ic/\omega ab)V$ and the transverse displacement current is $(2ia\omega/\pi bc)V$.[5] Propagation occurs at frequencies such that the displacement current exceeds the conduction current; cutoff occurs when the two are equal, *i.e.*, $\omega_c=\pi c/a$, as in (1) above. This criterion is, in fact, a way of defining cutoff in a waveguide. Similar relations hold in a plasma. The difference is essentially one of *geometry*. The conduction current and displacement current flow in the same volume in the plasma whereas the conduction current in a waveguide is confined to the walls while the displacement current is concentrated at the center.

The foregoing considerations indicate the possibility of simulating certain properties of inhomogeneous plasma by the use of waveguides with varying cross section. To analyze this possibility we find it convenient to use the radial waveguide (sectoral horn) configuration shown in Fig. 2(a), writing the wave equation in cylindrical coordinates:

$$\left[\frac{1}{r}\frac{\partial}{\partial r}\left(r\frac{\partial}{\partial r}\right)+\frac{1}{r^2}\frac{\partial^2}{\partial\theta^2}+\frac{\partial^2}{\partial z^2}+\left(\frac{\omega}{c}\right)^2\right]E_z=0. \quad (4)$$

We are interested in cylindrical waves that propagate in the radial direction and go over to the TE_{10} mode is rectangular waveguide as $r\to\infty$, in which case $\partial^2/\partial z^2=0$, $E_\theta=E_r=0$, $E_z\neq 0$.

Writing $E_z=R(r)\,\Theta(\theta)$, separating variables and making use of the fact that the tangential electric field must vanish at the walls ($\theta=\pm\alpha$), we obtain the azimuthal solution $\Theta=\cos(\pi\theta/2\alpha)$. The radial wave function is given by the Bessel equation

$$\frac{d^2R}{dr^2}+\frac{1}{r}\frac{dR}{dr}+\left[\left(\frac{\omega}{c}\right)^2-\frac{\mu^2}{r^2}\right]R=0, \quad (5)$$

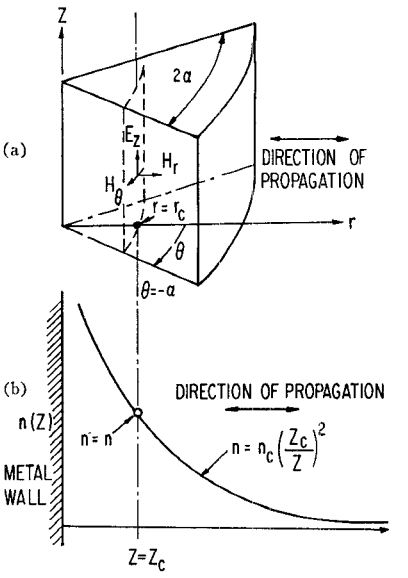

Fig. 2—(a) Tapered waveguide. (b) Equivalent plasma density distribution.

and the solution that remains finite at the origin is $R=J_\mu(kr)$ where $k=\omega/c$ and $\mu=2\pi/\alpha$. The quantity μ can also be written in terms of r_c, the "turning point," *i.e.*, the value of r at which the last term in (5) vanishes; the solution for the radial waveguide problem is then

$$E_z=AJ_\mu(kr)\cos\mu\theta \quad (6)$$

where $\mu=r_c/\lambda\!\!\!^{-}$ and $\lambda\!\!\!^{-}=\lambda/2\pi$.

We now consider the wave equation for propagation of TE waves in an inhomogeneous plasma whose density is a function of z only:

$$\nabla^2\boldsymbol{E}-\nabla(\nabla\cdot\boldsymbol{E})-\left(\frac{\omega}{c}\right)^2\epsilon(\omega,z)\boldsymbol{E}=0. \quad (7)$$

We are interested in propagation at normal incidence [Fig. 2(b)] so that $E_y=E_z=0$, $\partial/\partial x=\partial/\partial y=0$, $\nabla\cdot\boldsymbol{E}=\partial E_x/\partial x=0$; the effective dielectric constant for the inhomogeneous plasma is given by

$$\epsilon=\left[1-\frac{\omega_p^2(z)}{\omega^2}\right]=\left[1-\frac{n(z)}{n_c}\right]$$

where n_c is the critical density corresponding to a given ω and $n(z)$ is a function such that $n(z)=n_c$ at $z=z_c$.

Eq. (7) then becomes

$$\frac{d^2E_x}{dz^2}+\left(\frac{\omega}{c}\right)^2\left[1-\frac{n(z)}{n_c}\right]E_x=0. \quad (8)$$

Examination of (5) and (8) suggests that a correspondence can be established by writing $n(z)=n_c(z_c/z)^2$, in which case (8) becomes

$$\frac{d^2E_x}{dz^2}+\left[k^2-\frac{(z_c/\lambda\!\!\!^{-})^2}{z^2}\right]E_x=0 \quad (9)$$

which is the "normal" form of the Bessel equation, with general solution[6]

[3] J. D. Jackson, "Classical Electrodynamics," John Wiley and Sons, Inc., New York, N. Y., 1962.
[4] L. Spitzer, "Physics of Fully Ionized Gases," Interscience Publishers, Inc., New York, N. Y.; 1962.
[5] S. A. Schelkunoff, "Electromagnetic Waves," D. Van Nostrand Co., Inc., Princeton, N. J.; 1943.
[6] E. Jahnke and F. Emde, "Tables of Functions with Formulae and Curves," Dover Publications, Inc., New York, N. Y.; 1945.

$$E_x = A\sqrt{z}J_p(kz) + B\sqrt{z}J_{-p}(kz)$$

where

$$p = [(z_c/\lambda)^2 + 1/4]^{1/2} \geq 1/2.$$

Reference to the asymptotic expression[6]

$$\sqrt{z}J_{-p}(kz) \approx z^{1/2-p},$$

which holds for $z \to 0$, shows that this part of the solution must be rejected to obtain a finite solution at the origin, corresponding to the case in which the plasma is backed by a metal wall as in Fig. 2(b).[7] The solution for the plasma with the inverse quadratic density distribution is then

$$E_x = \sqrt{z}J_p(kz)$$

where $p \approx z_c/\lambda$ (assuming $z_c > \lambda$).

Now, comparing (6) and (10) (with $\theta = 0$) we see that the waveguide and plasma shown in Fig. 2 exhibit analogous behavior with respect to a TE wave propagating toward the origin. In particular, the wave undergoes "reflection" in the neighborhood of the critical density z_c or the critical cross section r_c. Similarly, an evanescent wave arises at the critical point and damps out toward the origin. Thus, analog experiments carried out with appropriate tapered-waveguide configurations appear to be useful for simulating inhomogeneous plasma media in the vicinity of critical densities. Such experiments would require slowly-varying taper structures in order to minimize effects due to generation of spurious modes at junctions with other microwave elements.

HERBERT LASHINSKY
Plasma Physics Lab.
Princeton University
Princeton, N. J.

[7] L. S. Taylor, "Reflection of a TE wave from an inverse parabolic ionization density," IRE TRANS. ON ANTENNAS AND PROPAGATION (*Correspondence*), vol. AP-9, pp. 582–583; November, 1961.

The Diffraction Loss Curve for Nonconfocal Spherical Mirrors

The diffraction loss curve vs Fresnel number for confocal spherical mirrors was shown by Fox and Li[1] and by Goubau and Schwering.[2] Boyd and Gordon[3] suggested a possibility of applying the above theory to a nonconfocal mirror system, by assuming the diffraction loss to be equal to that of an equivalent confocal system having the same spot size. They proposed to express the diffraction loss in term of the parameter

$$\frac{a'^2}{d\lambda}\left[2\frac{d}{b'} - \left(\frac{d}{b'}\right)^2\right]^{1/2}$$

in place of the conventional Fresnel number N.

The approximation by Boyd and Gordon has been found nearly valid by Fox and Li[4] for the range of $0.2b' < d < 1.8b'$ in the calculation of infinite strip curved mirror interferometers for $N = 0.5$.

Using the Boyd and Gordon approximation, the diffraction loss for a nonconfocal system may be expressed as a function of the above parameter, which can be modified to the form

$$N\left[2\left(\frac{b'}{d}\right) - 1\right]^{1/2}$$

where

b' = radius of curvature of mirrors
d = spacing between mirrors
N = Fresnel number $= a'^2/b'\lambda$
a' = radius of mirrors.

The above new parameter corresponds to the Fresnel number N for a confocal system, and the diffraction loss for a nonconfocal system can be easily obtained using the loss curve for a confocal system by replacing N to the form modified by the factor

$$\left[2\left(\frac{b'}{d}\right) - 1\right]^{1/2}.$$

On the other hand, it is sometimes required to calculate the variation of the diffraction loss for a nonconfocal system with the spacing between mirrors for constant mirror curvature and wavelength. In such a case, it seems more convenient to use the new parameter N' as defined by the formula

$$N' = \frac{a'^2}{d\lambda}.$$

With this parameter, the diffraction loss for a nonconfocal system can be illustrated for various values of N as shown in Fig. 1. The solid line in the figure denotes the loss curve for a confocal system for comparison. These curves seem to have sufficient accuracy in the range of $0.2b' < d < 1.8b'$.

When the diffraction loss for a nonconfocal system was measured for a variable mirror spacing, the measured value should be compared with the curve shown in Fig. 1, not with the loss curve for a confocal system. It is considered that the results of the measurement made by Beyer and Scheibe[5] may be compared more adequately with the curve in Fig. 1 for a given value of N.

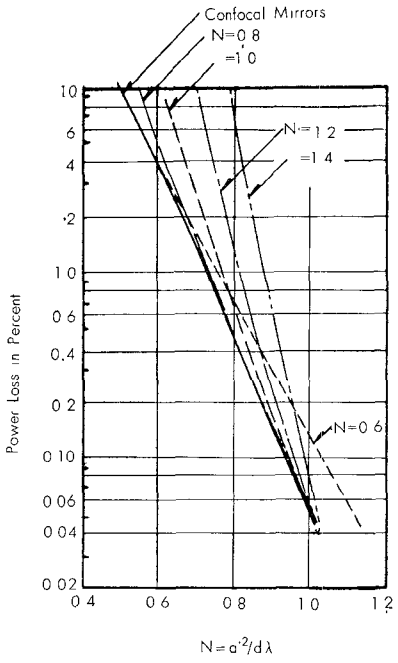

Fig. 1—Diffraction loss for a nonconfocal system of spherical mirrors.

ACKNOWLEDGMENT

The author wishes to thank Dr. F. Ikegami, the chief of the Second Radio Section in the Electrical Communications Laboratory for his support.

TAKEO OMORI
Electrical Communication Lab.
Nippon Telephone and Telegraph
Public Corp.
Tokyo, Japan

[5] J. B. Beyer and E. H. Scheibe, "Loss measurements of the beam waveguide," IEEE TRANS. ON MICROWAVE THEORY AND TECHNIQUES, vol. MTT-11, pp. 18–22; January, 1963.

Semiconductor Switching and Limiting Using 3-db Short-Slot (Hybrid) Couplers

The silver-bonded germanium varactor diode has been successfully used as a switch and a limiter of microwave power when operated in a series mode between 9.0 and 9.6 Gc.[1] This report gives details of shunt mode switching and limiting using these same type diodes in conjunction with 3-db short-slot (hybrid) couplers. The technique of using 3-db short-slot (hybrid) couplers, but with other type diodes (*e.g.*, 1N263, MA-450, PIN's), has been reported by other investigators.[2–4]

Fig. 1 is a diagrammatic illustration of the short-slot (hybrid) coupler. If arms B and C are terminated in perfectly matched

Manuscript received December 17, 1963.

[1] A. G. Fox and T. Li, "Resonant modes in a maser interferometer," *Bell Sys. Tech. J.*, vol. 40, pp. 453–488; March, 1961.

[2] G. Goubau and F. Schwering, "On the guided propagation of electromagnetic wave beams," IRE TRANS. ON ANTENNAS AND PROPAGATION, pp. 248–256; May, 1961.

[3] G. D. Boyd and J. P. Gordon, "Confocal multimode resonator for millimeter through optical wavelength masers," *Bell Sys. Tech. J.*, vol. 40, pp. 489–508; March, 1961.

[4] A. G. Fox and T. Li, "Modes in a maser interferometer with curved and tilted mirrors," PROC. IEEE, vol. 51, pp. 80–89; January, 1963.

Manuscript received December 19, 1963.

[1] V. J. Higgins, "X-band semiconductor switching and limiting using waveguide series tees," *Microwave J.*, vol. 6, pp. 77–83; November, 1963.

[2] R. Lucy, "Microwave High Speed Switch," *Proc. Natl. Electronics Components Conf.*, Philadelphia, Pa., pp. 12–15; May, 1959.

[3] R. V. Garver and D. Y. Tseng, "X-band diode limiting," IRE TRANS. ON MICROWAVE THEORY AND TECHNIQUES (*Correspondence*), vol. MTT-9, p. 202; March, 1961.

[4] W. F. Krupke, T. S. Hartwick and M. T. Weiss, "Solid-state X-band power limiter," IRE TRANS. ON MICROWAVE THEORY AND TECHNIQUES, vol. MTT-9, pp. 472–480; November, 1961.